PREPARATION OF INPUT AND VALIDATION DATA FOR PZL SW-4 HELICOPTER DYNAMIC MODEL IN SCOPE OF HELIMARIS PROJECT

Adam Rosłowicz
"PZL-Świdnik" S.A. Leonardo Helicopters Company Świdnik, Poland
E-Mail: adam.roslowicz@leonardocompany.com
Phone: +48 81 722 6332

Abstract
HELIMARIS project ("Modification of an optionally piloted helicopter to maritime mission performance") aims in preparation of maritime operation of PZL SW-4 helicopter. Due to operational and economic issues, it is a reasonable approach to simulate the most hazardous flight stages before proceeding to flight test. Warsaw University of Technology (WUT) developed PZL SW-4 helicopter dynamic model implemented in FLIGHTLAB environment in scope of HELIMARIS project. The model should represent actual performance and dynamics of helicopter in basic flight states (hover, cruise, climb/descent, turn, etc.). Compliance with this requirement allows to predict PZL SW-4 behavior in harsh maritime environment, especially focused on ship approach, in a reliable manner. Presented effort is complementary with analyses and laboratory tests done simultaneously by the other project subcontractor – Ship Design and Research Centre (CTO), which purpose is to obtain ship air wake and helideck motion data to be integrated in FLIGHTLAB environment. Investigation will result in definition of safe and efficient operational procedure for light maritime helicopter. The purpose of the paper is to present each particular phase of required input data preparation done by PZL-Świdnik (Original Equipment Manufacturer; OEM). Therefore, it provides necessary background for detailed control algorithms description and regulator system adjustment, performed by Warsaw University of Technology. PZL-Świdnik provided definition of mass, inertial and geometrical data set in basic helicopter configuration. This included geometry of main rotor hub, tail rotor hub, stabilizers and landing gear. Position of sensors, indicators and all relevant systems was defined. Main rotor system definition contains also damping characteristics of lag damper. Main rotor and tail rotor blades were defined in terms of necessary properties distribution (mass, inertia, chord). Aerodynamic characteristics of airfoils in entire range of section Mach number were verified and tailored in order to achieve flight test compliance. Static stiffness and strength of landing gear was obtained from stand test results, including also limits for landing conditions. Fuselage was defined in terms of aerodynamics. Due to high predicted angles of attack and sideslip in ship air wake, supplementation of already used characteristics was required. CFD (Computational Fluid Dynamics) ANSYS Fluent solver was employed to obtain missing data. Results were tailored to obtain compliance with existing characteristics in narrow range of inflow angles and with actual power required for flight. Fuselage aerodynamics is to be supplemented by floats once detailed configuration is available. Helicopter control system was defined in terms of kinematic ratio between controls and swashplate position. Kinematics of swashplate was supplemented by longitudinal/lateral feathering coupling and main rotor flap feathering coupling formulation. Dynamic characteristic of hydraulic actuators was also provided. PZL-Świdnik calculated vortex ring conditions envelope. Propulsion system definition was a distinct phase of dynamic model development. It included description of kinematic ratio between collective lever and engine control lever position. PZL-Świdnik provided detailed kinematics of engine controls and nominal engine control characteristics (nominal output power vs engine control lever position). Fuel system mass flow limits and tank capacity were based on PZL SW-4 Rotorcraft Flight Manual. Simultaneously, set of flight test data was prepared. Dedicated flight test program was prepared and performed. It contained measurements of state parameters relevant for dynamic identification in time domain and validation of the model. First of all, sign convention and measurement system characteristics were provided to obtain compliance and integrity with simulation results. Then, controls input signals were defined for dynamic response investigation. There were two types of inputs – long step and fast doublet. Two groups of dynamic response flight states were established: near-ground maneuvers (hover in-ground effect, hover off-ground effect, directional movements) and forward flights (level flight, climbing/descent, turns). Each contained both long step and fast doublet control input in every control channel (collective, longitudinal cyclic, lateral cyclic, pedals). General description of test helicopter configuration and external conditions were provided. Second stage of flight test was equilibrium conditions and control margins investigation. PZL-Świdnik provided detailed controls positon (swashplate pitch and roll), helicopter attitude (fuselage pitch and roll), and rotors collective angles in trimmed level flight. The same data set was prepared for autorotation. Static equilibrium conditions were compared with results obtained from own O50 FORTRAN code. The last group of static tests was in-ground controllability and maneuverability. It contains presentation of controls position vs wind azimuth. Distinct phase was a definition of static performance and dynamic characteristics of propulsion system. Static performance of RR M250-C20R/2 engine was calculated using Rolls-Royce application. Dynamic characteristic includes propulsion system time response in relevant flight states (start-up, vertical take-off, landing from high hover, entry into autorotation, recovery from autorotation). Dedicated on-ground propulsion system stability test was used for engine sub-model calibration. Initial validation of entire model was done with support of selected steady flight test data. Flight test data obtained from landings on a moving platform was used for initial definition of ship landing procedure. Approach and take-off profile were established. Data set contained state parameters measurements correlated with video recording of each particular approach. Additionally, influence of control chain dynamic stiffness and slack of the controls was assessed. Swashplate position calibrated from controls was compared with that calculated kinematically from actuator extension. MATLAB script was employed to calculate transfer function between actuators extension and swashplate position and to compare with flight measurements of actuator forces. Static slack of the controls was defined from stand tests. PZL provided also qualitative and quantitative criteria for dynamic model similarity assessment for both dynamic response and static equilibrium part.

Presented at 45th European Rotorcraft Forum, Warsaw, Poland, 17-20 September, 2019

These were defined in terms of simulation results as follows: response vector signs compliance, attitude deviation from measurement at certain time from input signal beginning, controls position difference in trimmed steady flight. A vital phase of the project is PZL SW-4 autopilot sub-model development. It required detailed definition of sub-system functionality, general architecture, emergency scenarios, requirements and limitations. Autopilot sub-model should allow to perform basic flight states in whole PZL SW-4 operational envelope with Stability Augmentation System (SAS) functionality. Additional automatic flight modes will be tailored to support wide spectrum of maritime missions in both manned and unmanned configuration. The most critical phase is automatic vertical take-off and landing with sea state up to 5. Manual landing procedure will be extensively examined during simulation campaign.

1. SYMBOLS AND ABBREVIATIONS

AoA	Angle of Attack
CAD	Computer Aided Design
CFD	Computational Fluid Dynamics
CoG	Center of Gravity
FD	Fast Doublet
h/c	helicopter
IAS	Indicated Airspeed
IGE	In-Ground Effect
IMU	Inertial Measurement Unit
LS	Long Step
MR	Main Rotor
MTOW	Maximum Take-Off Weight
OAT	Outside Air Temperature
RFM	Rotorcraft Flight Manual
TOT	Turbine Outlet Temperature
TOW	Take-Off Weight
TR	Tail Rotor
WUT	Warsaw University of Technology

Symbols are declared in body text. In case of italics, they refer to PZL own nomenclature; bolded refer to FLIGHTLAB nomenclature.

2. INTRODUCTION

PZL SW-4 helicopter dynamic model is being built in scope of HELIMARIS project ("Modification of an optionally piloted helicopter to maritime mission performance"). Nowadays, complex and advanced simulation tools are widely employed in aerospace industry to predict performance and dynamic behavior in the most hazardous flight states. As far as maritime operation is considered, it covers such states as entrance into turbulent ship air wake, close approach to helideck and final descent. In HELIMARIS project, FLIGHTLAB simulation environment integrates helicopter dynamic model, external conditions and ship dynamic model. Thanks to its intuitive, user friendly interface, it allows to build and modify object dynamic model in far more easier manner. That constitutes profound advance compared with particular, specific purpose own applications, previously used in PZL.

The paper summarizes all necessary stages of dynamic model preparation. Firstly, it covers mass, balance and geometrical data as well as detailed characteristics of helicopter sub-systems. Secondly, flight test description, dynamic identification strategy and static equilibrium is provided. Particular dynamics and static performance of engine sub-system is also to be defined. The main difficulties, which emerged during data implementation and interpretation by WUT, will be highlighted.

Further effort of WUT includes optimization of ship landing procedure. It is desired to provide an initial approach trajectory and helicopter dynamics during particular maneuvers. PZL flight test data from moving platform landing will be employed to support this task.

Dynamic model behavior should be assessed by objective numeric criteria. It is necessary by PZL to provide overall assessment methodology.

The last stage of model development will be autopilot sub-model implementation. That is a vital part of the whole effort. Harsh maritime environment implies need of pilot support and stability augmentation. PZL is to provide functionality description, emergency scenarios definition, requirements and helicopter operational limitations, which auto-pilot should follow.

3. INPUT DATA PREPARATION

The chapter summarizes all input data required in FLIGHTLAB environment to build object dynamic model. The most challenging and influencing issues were widely discussed. The chapter presents data obtain methodology, format and values itself in a qualitative manner. Figure 1 shows general helicopter dimensions.

Presented at 45th European Rotorcraft Forum, Warsaw, Poland, 17-20 September, 2019

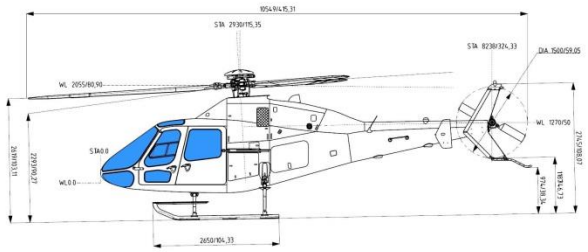

Figure 1. General PZL SW-4 dimensions.

3.1. Helicopter coordinate system

Position and dimensions were defined in basic design reference system obtained from intersection of:

- H/c symmetry plane;
- Basic horizontal assembly plane (corresponding to floor level in the cabin);
- Plane of 11th fuselage frame.

3.2. Weight and balance

Weight and balance definition is crucial, when such issues like: power required for flight, control margins as well as dynamic responses are concerned. It was decided to provide both limiting configurations in terms of helicopter mass and longitudinal CoG position (see Table 1). The lightest one (CONF0) corresponds to minimum equipped helicopter with crew onboard and required mission payload. The mean configuration (CONF1) was chosen to be close to majority of flight tests. The heaviest one (CONF2) corresponds to MTOW.

3.3. Main rotor

Main rotor was defined in terms of general, global parameters. List of declared symbols is not exactly the same, due to differences in kinematics modeling between PZL own aero-mechanics code and FLIGHTLAB.

- hub center position **fsmr, blmr, wlmr**;
- main shaft tilt angle D_{FK} / **eulerhub**;
- number of blades Z / **nblades**;
- nominal rotor rotational speed P_{nom} / **rpmnom**;
- rotor radius R_W / **rmr**;
- rotor swashplate phase angle **phase**;
- rotor precone **coneang**;
- precone offset from rotor rotational center **coneof**;
- blade offset from rotation center in lag direction **transylen**;
- flapping hinge offset from rotational center l_{ph} / **flaphof**;
- lag hinge offset from rotational center l_{pv} / **laghof**;
- feathering hinge offset from rotational center r_{p0} / **feathof**;
- δ_3 angle for flap-pitch coupling[2] ξ_z / **delta3**;
- damping characteristic of lag damper (lag hinge damping moment vs lag hinge angular speed) εM_{TL} / **lagdamper**.

In order to confirm correct implementation of MR hub kinematics, PZL provided blade pitch angle formulation[1]:

(1) $$\varphi_1 = -\bar{D}_1\kappa + \bar{D}_2\eta$$

(2) $$\varphi_2 = \bar{D}_1\eta + \bar{D}_2\kappa$$

(3) $$\varphi(\psi) = \varphi_0 - \varphi_1 \sin\psi - \varphi_2 \cos\psi - k_H\beta(\psi)$$

where:

φ_1, φ_2 – swashplate longitudinal and lateral angles;

$\bar{D}_1, \bar{D}_2$ - rotor vs swashplate longitudinal and lateral kinematical coupling;

κ - swashplate pitch angle;

η - swashplate roll angle;

ψ - blade azimuth;

k_H - flap-feathering coupling coefficient;

β - flapping angle.

Non-dimensional kinematical coupling coefficients were calculated from MR hub dimensions:

(4) $$\bar{D}_1 = \frac{R_{a,\pi}}{l_\pi}\cos\left(\sigma_\pi - \Delta\psi_{y\pi p} - c_0\right)$$

(5) $$\bar{D}_2 = \frac{R_{a,\pi}}{l_\pi}\sin\left(\sigma_\pi - \Delta\psi_{y\pi p} - c_0\right)$$

Input parameters in eq. 4-5 are defined on Figure 2.

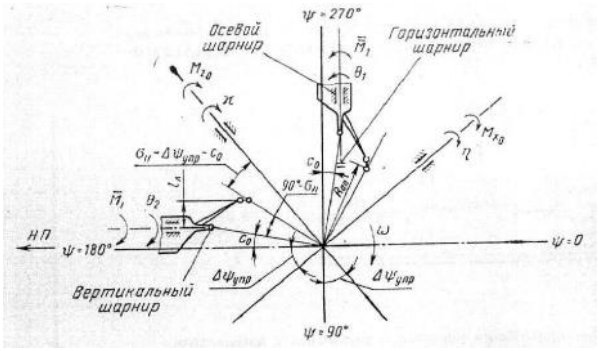

Figure 2. MR hub kinematics.

MR blade structure was defined in terms of mass and geometrical properties of finite elements (sections):

- end radius r / **mrbrad**;
- chord b / **bchord**;
- twist $\Delta\varphi$ / **btw**;
- chord-wise CoG offset from elastic axis σ / **bcgo**;
- moment of inertia about the pitch axis I_m / **bsegixx**;
- moment of inertia about the roll axis **bsegiyy**;
- moment of inertia about the yaw axis **bsegizz**;
- mass m / **bmpl**;
- offset of mid-chord from elastic axis **bsege0**;
- blade tip sweep **bsweep**;
- blade tip droop **bdroop**.

The last part of MR data are aerodynamic characteristics of blades. These are based on common NACA23012 airfoil, which was slightly modified

Presented at 45th European Rotorcraft Forum, Warsaw, Poland, 17-20 September, 2019

to represent actual performance of the rotor. Input parameters are:

- section drag coefficient *CX* / **mrcd**;
- section lift coefficient *CY* / **mrcl**;
- section pitching moment coefficient relative to 0.25*b* axis **mrcm025**.

Provided data covers entire range of operational Mach numbers and AoA.

3.4. Tail rotor

TR data provided is consistent with MR data listed in 3.3. Differences are:

- hub center position **fstr, bltr, wltr**;
- main shaft tilt angle D_{FK} / **eulerhubtr**;
- rotor radius **rtr**;
- flapping hinge offset from rotational center **aphof**;
- there is no lag damper.

Some flight tests do not include direct TR pitch angle measurement. In such cases, it could be calculated as linear function of TR pitch rod travel.
PZL own O50 code, employed to calculate h/c static equilibrium, does not require TR aerodynamic characteristics, since TR blade pitch angle is determined from Glauert-Lock theory[1]. However, FLIGHTLAB data provided is respectively:

- section drag coefficient **trcd**;
- section lift coefficient **trcl**;
- section pitching moment coefficient relative to 0.25 chord axis **trcm025**.

3.5. Propulsion system

The chapter contains listing of necessary input data referring to Rolls-Royce M250-C20R/2 turboshaft engine and transmission.

- Nominal speed of engine output shaft;
- Effective drivetrain rotary inertia **Ishaft**;
- MR gear ratio **GearKm**;
- TR gear ratio **GearKt**;
- Effective elastic torsional stiffness **Ktorsion**.

Definition of engine control system was essential for compliance with actual propulsion and rotors dynamics. There are two engine control modes. Once engine power lever is set to “GROUND IDLE” position, engine control system maintains fuel flow rate constant. Thus, output shaft speed is resultant and depends on external conditions and transmission resistance. In second mode (“AUTO”) power turbine governor is linked with MR collective lever. Output shaft speed is than maintained constant, at level set on trimming stick. Figure 3 shows general overview of engine control chain. Engine control mode is set by engine power lever (p. 13.).

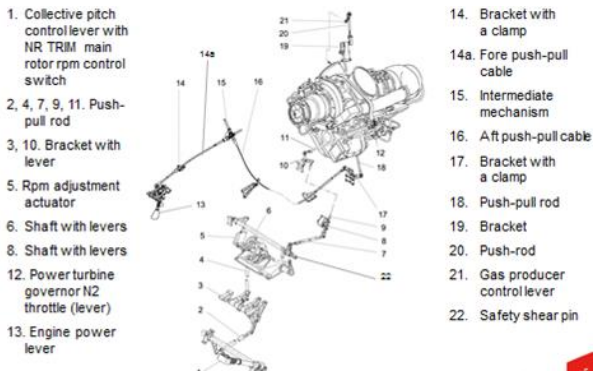

Figure 3. General description of engine control system.

Figure 4 shows nominal engine control characteristic. Output power is relative to take-off power. Power lever angle is relative to nominal maximum angle.

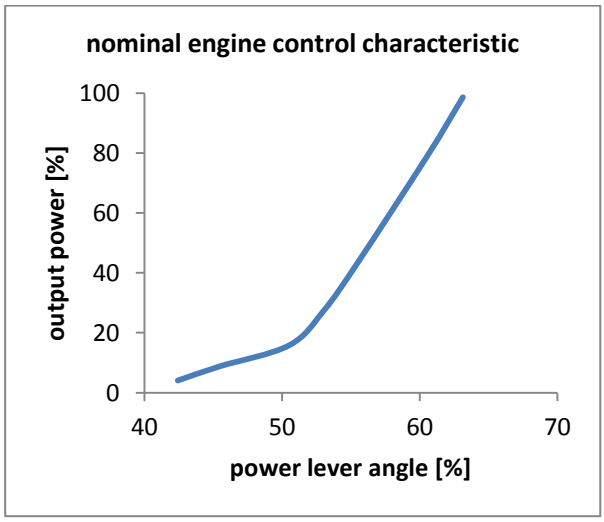

Figure 4. Nominal engine control characteristic.

Kinematic ratio between collective lever and power lever is provided in Table 2. All values provided are related to maximum.

Engine data was supplemented by weights of fuel and flow rates:

- Total initial fuel mass (max);
- Low fuel limit (caution);
- Out of fuel limit;
- Minimum fuel flow rate (ground idle);
- Maximum fuel flow rate (takeoff 5min).

3.6. Airframe

The chapter contains all relevant data referring to PZL SW-4 fuselage, aerodynamic surfaces, landing gear and control system. There is a definition of necessary characteristics of components.

Presented at 45th European Rotorcraft Forum, Warsaw, Poland, 17-20 September, 2019

3.6.1. Fuselage aerodynamics

Development of h/c dynamic model proceeded by WUT stated clearly, that reliable aerodynamic characteristics of fuselage are crucial. It profoundly affects object dynamics. Preparation of necessary data was divided on two major phases. Firstly, aerodynamic coefficients currently employed in PZL O50 code were provided to WUT. They were used for initial model development in basic flight states (forward flight). Due to O50 model assumptions, there are some important limitations. They cover narrow range of inflow angles:
Angle of attack: *ALK*; *ALKF*
Sideslip angle: *ABET*
Drag and lift coefficients are in fact only AoA dependent. Entire list of provided values consists of:
ALK - helicopter fuselage AoA vector [deg];

CXK - helicopter fuselage drag values vector relative to MR area for defined above fuselage AoA [-];

CYK - helicopter fuselage lift values vector relative to MR area for defined above fuselage AoA [-];

AMZK - helicopter fuselage pitch moment values vector relative to MR area for defined above fuselage AoA [-];

AMXK - table of fuselage roll moment coefficients for particular sideslip angles and particular fuselage AoA [-];

AMYK - table of fuselage yaw moment coefficients for particular sideslip angles and particular fuselage AoA [-];

ACZK - table of fuselage side force coefficients for particular sideslip angles and particular fuselage AoA [-];

DAMZK - table of fuselage pitch moment coefficients increment for particular sideslip angles and particular fuselage AoA [-];

DABETK - table of vertical stabilizer inflow angles for particular sideslip angles and particular fuselage AoA [deg];

ABET - fuselage sideslip angles vector [deg];

ALKF - fuselage angles of attack vector for *AMXK, AMYK, ACZK, DAMZK, DABETK* [deg].

Provided characteristics of fuselage include vertical stabilizer. That assumption implied different approach in TR FLIGHTLAB modelling, because it was not possible to engage vertical stabilizer interference explicitly. First phase moment coefficients refers to point close to h/c medium configuration (CONF1). O50 aerodynamic characteristics are presented on Figure 5 to Figure 9.

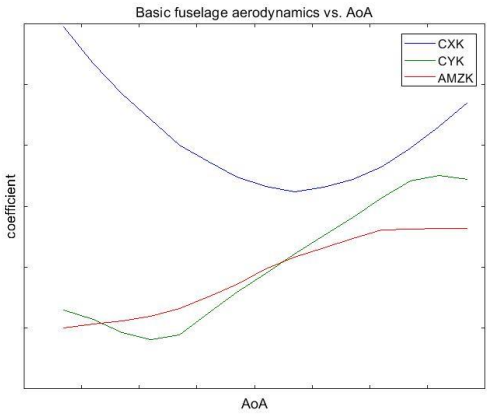

Figure 5. Basic fuselage aerodynamic characteristics with no sideslip.

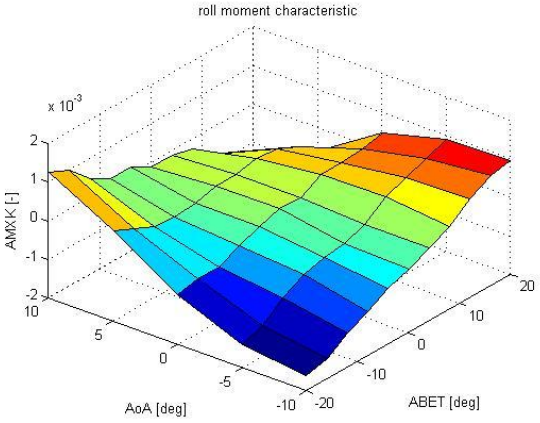

Figure 6. Basic roll moment characteristic.

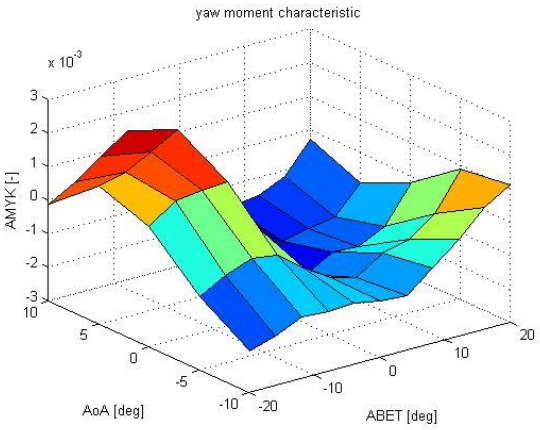

Figure 7. Basic yaw moment characteristic.

Presented at 45th European Rotorcraft Forum, Warsaw, Poland, 17-20 September, 2019

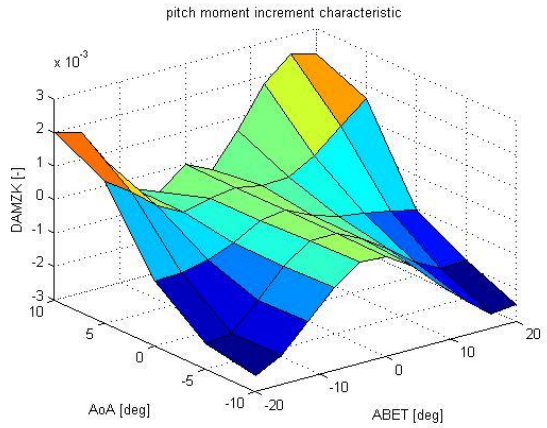

Figure 8. Basic pitch moment increment characteristic.

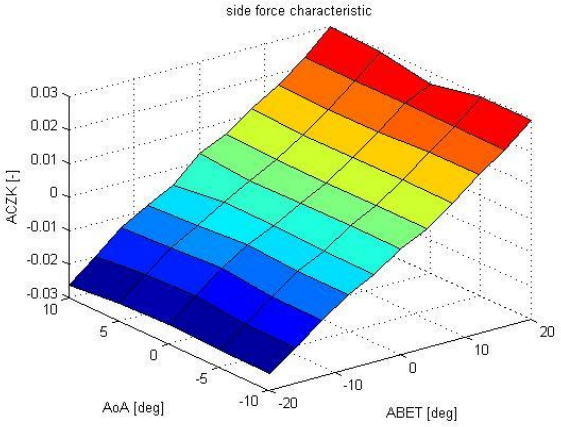

Figure 9.Basic side force characteristic.

Basic aerodynamic characteristics of fuselage do not allow to reflect h/c equilibrium conditions and dynamics in full range of flight states. It refers especially to maritime operation including approach to ship in turbulent air wake and hover over helideck. Strong turbulence in such conditions implies high AoA and sideslip angle. Therefore, it was necessary to provide WUT complete range of inflow angles. To comply with this requirement, CFD ANSYS Fluent solver was employed. Description of PZL SW-4 model assumptions was provided in [3]. Figure 10 shows general model overview, coordinate system and static pressure distribution on the fuselage in one computational case.

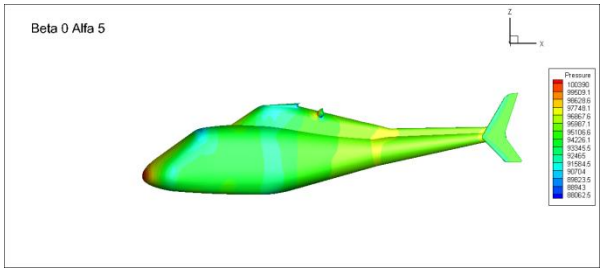

Figure 10. CFD model of PZL SW-4.

Full range aerodynamics data contains coefficients of six components (lift, drag, side force, pitch moment, roll moment, yaw moment). They were provided in tabular form as a function of AoA and sideslip angle. Coefficients of moments refers to MR hub center. It was necessary to post-process direct CFD results, in order to obtain smooth input data to be implemented in FLIGHTLAB. Thus, some numeric discontinuities which could result in FLIGHTLAB convergence difficulties, were avoided. Side force coefficients in the most numerically challenging cases were obtained as linear interpolation in AoA domain. Finally, forces and roll moment coefficients were smoothed using two methods:

- Moving average filtering in AoA domain using a fixed window length w that is determined heuristically. For a smoothing factor τ, the heuristic estimates a moving average window size that attenuates approximately 100τ percent of the energy of the input data.

(6)
$$\begin{cases} C_{smooth}(j_1, j_2) = \frac{1}{w}\sum_{k=j_2-b}^{j_2+b} C(j_1, k) \\ b = \left\lfloor \frac{w}{2} \right\rfloor \end{cases}$$

MATLAB `smoothdata` function was employed.

- convolution in sideslip angle domain defined as:

(7)
$$\begin{cases} C_{smooth}(j_1, j_2) = \sum_{k=j_1-b}^{j_1+b} C(k, j_2)s \\ s = \frac{[1]_{w\times 1}}{w} \\ b = \left\lfloor \frac{w}{2} \right\rfloor \end{cases}$$

MATLAB `convn` function was employed. “Same” shape was chosen, which returns the central part of the convolution.

Final, complete aerodynamic characteristics are presented on Figure 11-Figure 16.

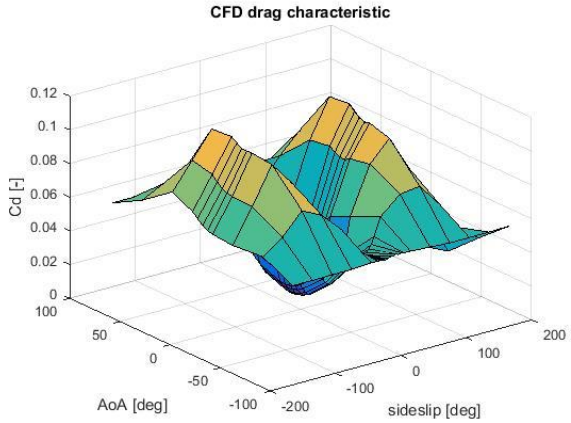

Figure 11. Complete drag characteristic.

Presented at 45th European Rotorcraft Forum, Warsaw, Poland, 17-20 September, 2019

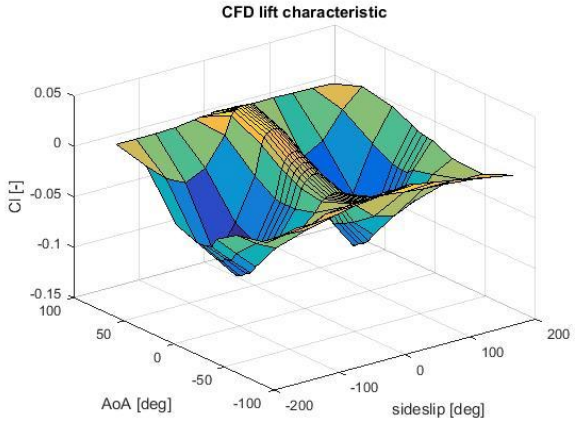

Figure 12. Complete lift characteristic.

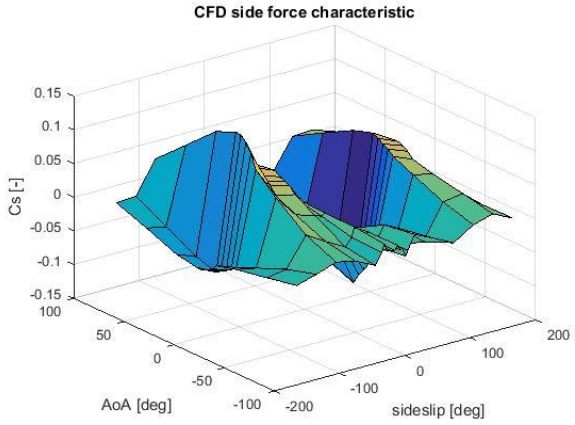

Figure 13. Complete side force characteristic.

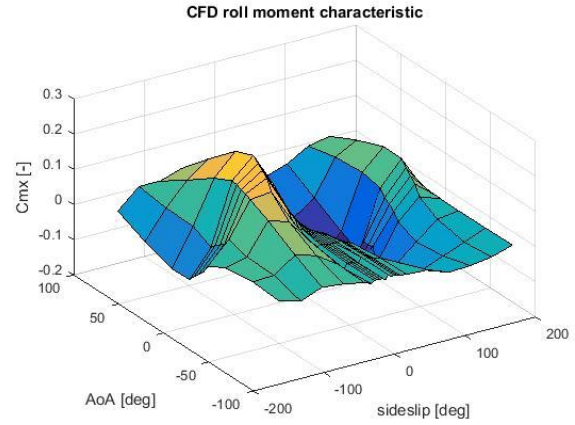

Figure 14. Complete roll moment characteristic.

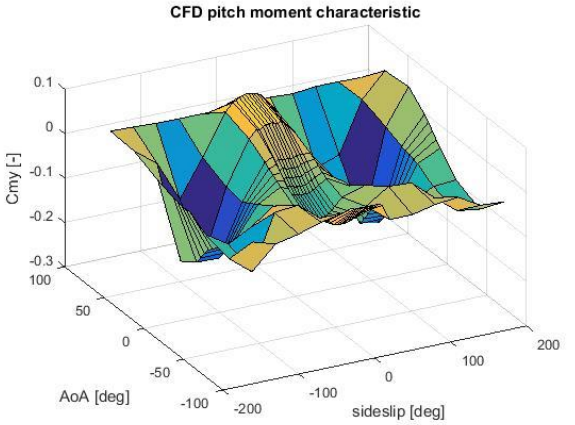

Figure 15. Complete pitch moment characteristic.

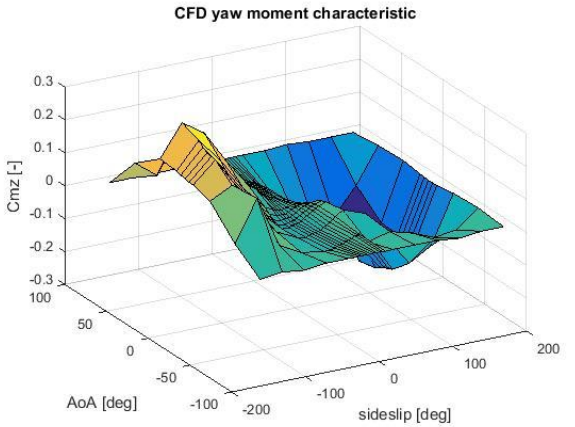

Figure 16. Complete yaw moment characteristic.

Fuselage aerodynamics was supplemented by position of aerodynamic center:

- fuselage station of fuselage aero center **fswf**;
- buttline station of fuselage aero center **blwf**;
- waterline station of fuselage aero center **wlwf**.

3.6.2. Stabilizers and end-plates

Stabilizing surfaces were defined in terms of necessary dimensions, position and aerodynamics. Table 3 lists input FLIGHTLAB parameters.
PZL provided aerodynamic characteristics of isolated horizontal stabilizer, vertical stabilizer and end-plates. In case of horizontal stabilizer, they consist of lift and drag:

ALSP - horizontal stabilizer angles of attack vector (15 values) [deg];

CYSP - horizontal stabilizer section lift coefficients vector (15 values) [-];
CXSP - horizontal stabilizer section drag coefficients vector (15 values) [-].
It corresponds with reversed NACA23012 airfoil.
Other surfaces were defined only in terms of side force:

ALSV - Vertical stabilizer local angle of attack [deg];
CZSV - Vertical stabilizer lift (side) force coefficient [-];

Presented at 45th European Rotorcraft Forum, Warsaw, Poland, 17-20 September, 2019

CZSP - Vertical stabilizing plate lift (side) force coefficient [-].

Due to low Mach number, compressibility effects were neglected. Values are presented on Figure 17 and Figure 18.

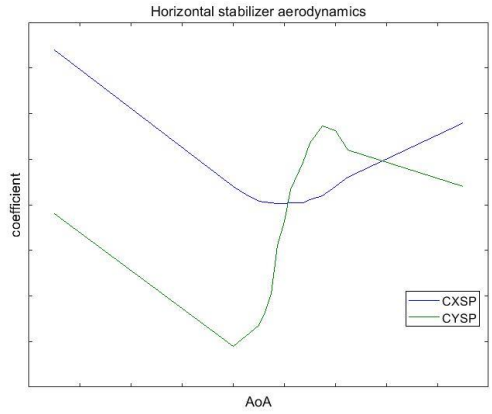

Figure 17. Horizontal stabilizer aerodynamic characteristic.

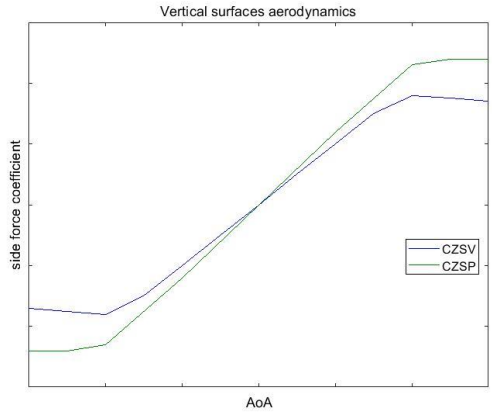

Figure 18. Vertical surfaces aerodynamic characteristics.

3.6.3. Sensors

PZL provided position of aerodynamic and inertial sensors, which was relevant for correct interpretation of flight test results and model calibration. That include position of both IMU employed in flight test campaign. Basic MGW-1SU provides only accelerations. Therefore, measurement system was supplemented by Crossbow AHRS-400CC-200 CM, which computes also time integrals to obtain angular velocities and attitude. Information include also position of altitude radar antenna and slip ball data. Furthermore, data set was supplemented by pilot eye position estimation. Complete list of sensors consist of:

- Primary IMU Crossbow AHRS-400CC-200 CM;
- Secondary IMU MGW-1SU;
- Fuselage g-load sensor (vertical acceleration);
- Slip ball;
- Pitot-static tube;
- Altitude radar.

FLIGHTLAB inputs are CS coordinates:

- fuselage station of i-th sensor OX – **fssensori**;
- waterline station of i-th sensor OY - **wlsensori**;
- buttline station of i-th sensor OZ - **blsensori**.

3.6.4. Landing gear

Landing gear was defined in terms of its static characteristic (deflection vs static load) and limitations. They include maximum crosstube load and landing conditions limitations (maximum landing field inclination, maximum landing velocity). Landing field inclination was demonstrated during prior flight tests. Maximum landing velocity was estimated from results of certification stand drop tests. Maximum touchdown velocity, at which no plastic deformation occurred, was chosen. Figure 19 and Figure 20 presents static characteristic of landing gear for two values of friction coefficient μ.

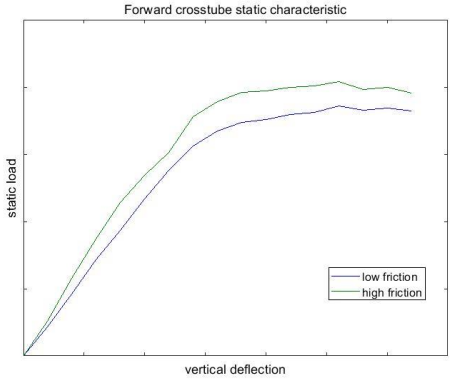

Figure 19. Forward crosstube static characteristic.

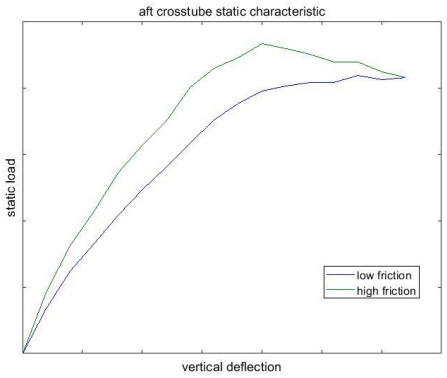

Figure 20. Aft crosstube static characteristic.

Skid landing gear model is not implemented into FLIGHTLAB environment. Thus, there is a need of translation of parameters to existing wheel-type model. Final model is calibrated to represent actual landing gear stiffness. Tail skid was also modelled as tail wheel, assuming common steel stiffness. Damping data was not provided, because on-ground phenomena (eg. ground resonance) are beyond scope of the project.

Presented at 45th European Rotorcraft Forum, Warsaw, Poland, 17-20 September, 2019

3.7. Control system

Definition and reliable modeling of h/c control system has crucial impact of its dynamic behavior. Nominal kinematic ratio between controls and final control elements was defined as follows:

- MR swashplate pitch vs longitudinal cyclic stick deflection;
- MR swashplate roll vs lateral cyclic stick deflection;
- MR collective vs collective lever deflection;
- TR collective vs pedals deflection.

PZL SW-4 has hydraulically augmented MR control system. Thus, actuators performance was provided:

- Ratio input/output – **rioa**;
- Dead stroke – **dsta**;
- Maximum deviation at output position with and without hydraulic pressure in a fixed position of input lever – **deva**;
- Actuator length in nominal position - **lmeda** (it is equivalent to the medium position of MR swashplate: pitch κ=0, roll η=0, collective on MR blade grip $\varphi=0.5\varphi_{max}$);
- Max. actuator rod stroke – **dla**;
- Stall load – **Fstall**;
- Min. actuator stroke speed guaranteed for zero load – **dva;**
- Max. actuator control input force guaranteed:
    - for low speed - Fmax_low;
    - for high control speed - Fmax_high;
- The lowest natural frequency of actuator - fmin.

Actuator dynamics is presented on Figure 21.

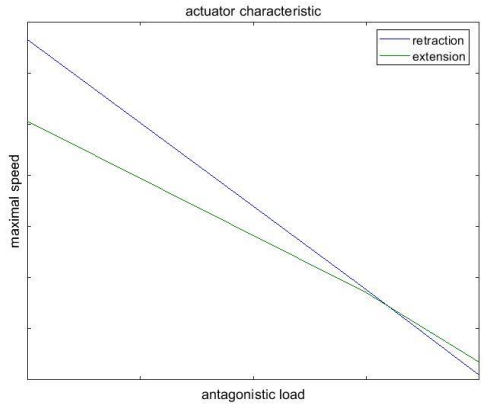

Figure 21. Actuator dynamics.

MR control system was supplemented by necessary swashplate dimensions:

- rotating part radius – **rswr**;
- non-rotating part radius – **rswn**;
- basic length of pitch rod - **lpcr**.

4. VALIDATION DATA

The chapter contains description of flight test data necessary for model validation. Definition of inputs, measured signals, flight states, h/c configuration and external conditions were provided. Then, some examples of responses are presented. Steady-state flight results in h/c attitude and final control elements position. Particular sub-chapters are focused on the most relevant tests. That refers to engine validation data, control chain dynamics and platform landing.

4.1. Dynamic response

PZL-Świdnik performed dedicated flight tests program aiming in dynamic identification. Time domain identification methodology was chosen. That allowed to reasonably represent object dynamics in wider range of control. Time domain identification is suitable for large disturbances and nonlinear models development, as implemented in FLIGHTLAB[4].
Dynamic response tests were performed in steady-state flight conditions. After stabilization of relevant flight parameters (velocity, climb speed, altitude, etc.), pilot maintained steady flight for at least 3s. Then, h/c was disturbed by controls inputs. No pilot reaction was applied in a period of 3s after end of control input, in order to examine h/c dynamic response.
Each test included application of disturbance in single control channel (longitudinal cyclic stick, lateral cyclic stick, collective lever, pedals).

4.1.1. Control inputs definition

The helicopter dynamic responses were examined by providing control signals, as defined below:

- Cyclic stick movement – left/right/forward/backward;
- Collective lever – down/up;
- Pedals – left/right forward.

Two control input profiles were used: “Long Step” (LS) and “Fast Doublet” (FD). Definition of input profiles and investigation methodology is presented on Figure 22 and Figure 23.

H/c dynamic model examination performed in FLIGHTLAB by WUT is based on actual, measured control signals. In real flight test conditions, pilot did not always follow defined investigation strategy exactly. Test phases duration and control input amplitude differs from each other in some cases. Therefore, there is a need of closer analysis of each particular flight case before applying it to simulation. WUT performed necessary overlook and choose cases best matching defined profile.

Presented at 45th European Rotorcraft Forum, Warsaw, Poland, 17-20 September, 2019

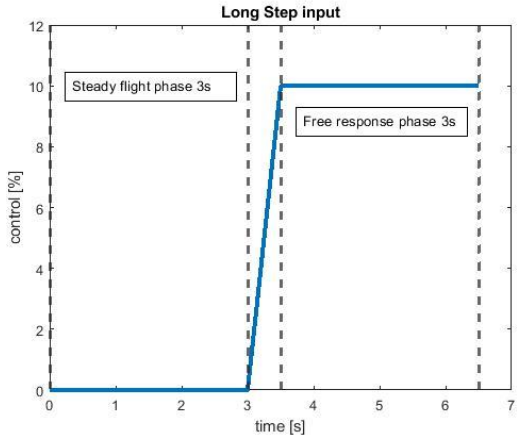

Figure 22. LS investigation methodology.

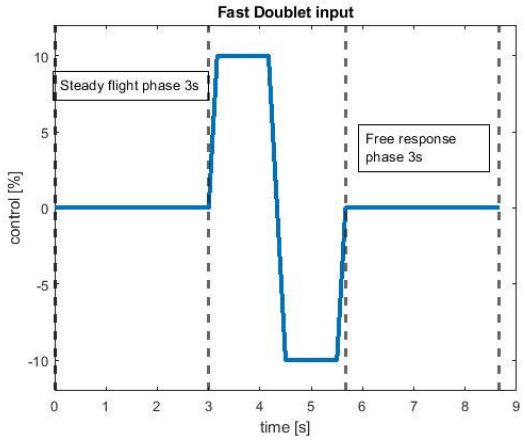

Figure 23. FD investigation methodology.

4.1.2. Measured parameters

The subchapter lists all parameters relevant in terms of flight tests interpretation. That include state parameters, external conditions, h/c position, navigation data. Some signals are redundant, due to multiple measuring systems. In case of inertial signals, Crossbow IMU data was defined as primary source, due to higher sampling rate and direct signals integration. Table 4 presents listing of measured signals. Near all signals in non-rotating frame were measured with constant, basic sampling frequency f_s. Basic MR speed counter had sampling frequency 25-times smaller. Signals in rotating frame (no. 505.0 and 504.0) were sampled with 4-times higher rate. Low passing analogous filter, with cut-of frequency of 0.25 of sampling rate, was applied to all signals (except of 988.0).

4.1.3. Flight states

H/c dynamics was investigated in following flight states, which covers all basic maneuvers:

- Hover IGE and OGE;
- Near ground maneuvers:
  - Forward movement;
  - Side movement right;
  - Side movement left;
  - Backward movement;
  - Vertical descend;
- Level flight at various IAS;
- Climbing and descend at various IAS.

In general, every flight state included control input in every channel and direction. Each case was repeated at least twice, in order to select better matching with theoretical assumptions.
Each flight was supplemented with corresponding h/c configuration (TOW, **fscg**), MR speed and external conditions (pressure altitude and wind).

4.2. Engine response

In order to reliably assess propulsion sub-system dynamics (time constant, damping decrement), there was a dedicated ground test. Engine was running in "AUTO" mode with collective in bottom position and trimming stick in neutral. Then, impulse response was investigated[5], by switching power lever to "GROUND IDLE" and immediately returning to "AUTO". General overview of engine response is shown on Figure 24.

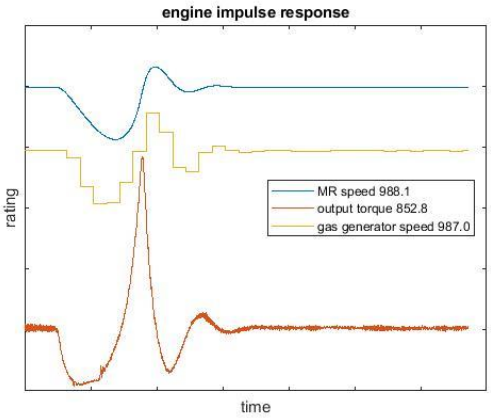

Figure 24. Engine impulse response test.

4.3. Control chain dynamics and slack

Basic, nominal kinematic ratio between controls and final control elements was provided, assuming ideally stiff control chain. However, there was a need to assess influence of control chain dynamics. Measurement of swashplate actuator rod extension was employed. Firstly, analytical non-linear relation between swashplate angles (κ, η, φ) and rods extension $L_{TW1,2,3sp}$ was derived from MR control system kinematics:

$$L_{TW1sp} = \sqrt{r_{a\varphi\kappa}^2 + \left(\Delta S_\varphi + \sqrt{l_{0\varphi\kappa}^2 - r_{a\varphi\kappa}^2}\right)^2} - l_0 \quad (8)$$

$$L_{TW2sp} = \sqrt{r_{a\varphi\eta}^2 + \left(\Delta S_\varphi + \sqrt{l_{02\varphi\eta}^2 - r_{a\varphi\eta}^2}\right)^2} - l_0 \quad (9)$$

$$L_{TW3sp} = \sqrt{r_{a\varphi\eta}^2 + \left(\Delta S_\varphi + \sqrt{l_{03\varphi\eta}^2 - r_{a\varphi\kappa}^2}\right)^2} - l_0 \quad (10)$$

where intermediate parameters are:

Presented at 45th European Rotorcraft Forum, Warsaw, Poland, 17-20 September, 2019

(11) $$l_{0\varphi\kappa} = \sqrt{r_{a\varphi\kappa}^2 + \left(\sqrt{l_0^2 + r_a^2} + r\sin\Delta\kappa\right)^2}$$

(12) $$l_{02\varphi\eta} = \sqrt{r_{a\varphi\eta}^2 + \left(\sqrt{l_0^2 + r_a^2} + r\sin\Delta\eta\right)^2}$$

(13) $$l_{03\varphi\eta} = \sqrt{r_{a\varphi\eta}^2 + \left(\sqrt{l_0^2 + r_a^2} - r\sin\Delta\eta\right)^2}$$

(14) $$r_{a\varphi\kappa} = r_a - r + r\cos\Delta\kappa$$

(15) $$r_{a\varphi\eta} = r_a - r + r\cos\Delta\eta$$

(16) $$\Delta S_\varphi = \Delta\varphi_{MR} k$$

Δκ, Δη, $\Delta\varphi_{MR}$ – swashplate pitch, roll and collective increment from neutral;
k – kinematic ratio between collective increment and swashplate travel.
Secondly, matrix of $L_{TW1,2,3sp}$ values corresponding with entire range of swashplate control was calculated from eq. (8)-(10).
Then, transfer functions K, E, F between $L_{TW1,2,3sp}$ and swashplate angles κ, η, φ were formulated with use of MATLAB `scatteredInterpolant` procedure.
Finally, obtained transfer functions K, E, F were employed to calculate swashplate angles from actual actuator extensions signals measured in flight. Results were compared with standard swashplate alignment signals, obtained from simple kinematic coupling with pilot controls. Difference was evaluated against actuator load, to assess influence of control chain stiffness. Additionally, mean value of swashplate angles difference in each flight state was subtracted, to eliminate influence of numeric and measurement accuracy. Thus, only dynamic effects were distinguished. Example of calculation in single flight state is shown on Figure 25.

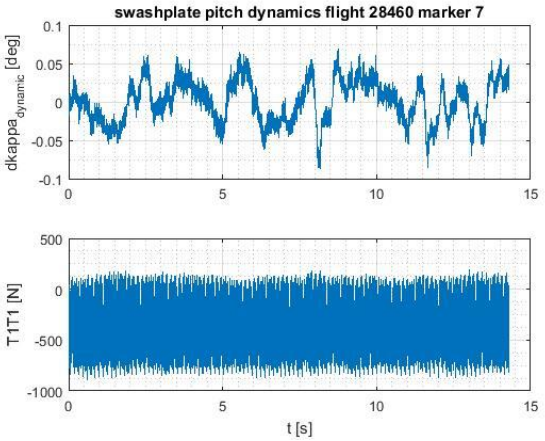

Figure 25. Dynamic swashplate pitch difference vs. actuator load.

Analysis showed, that control chain stiffness has no significant impact on swashplate angles measurement accuracy, in standard control system operation and external load.
Control chain slack was defined basing on ground test. It was not implemented in the model at the current stage of the project.

4.4. Steady-state equilibrium conditions

The chapter presents second part of validation data. It provides h/c attitude, swashplate angles and TR collective in steady-state flight.

4.4.1. Forward flight

Forward flight case was defined in terms of h/c configuration (weight, MR speed, CoG position) and extremal conditions (pressure altitude, OAT). Figure 26 presents swashplate equilibrium pitch angle in trimmed level flight for two CoG, as an example of provided data. It is compared with results of O50 code calculation shown on Figure 27.

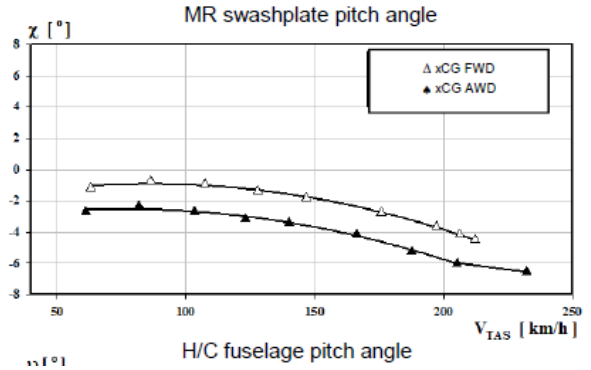

Figure 26. MR swashplate equilibrium pitch in level flight test.

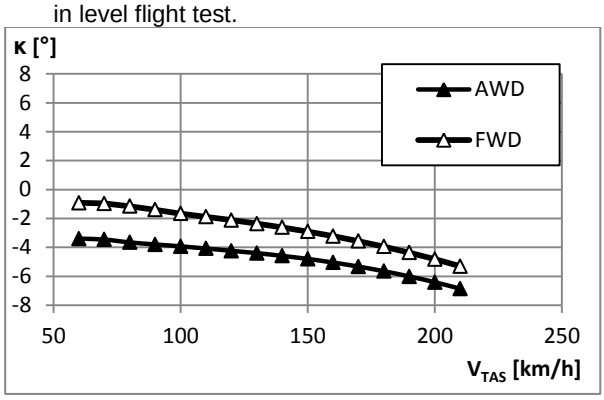

Figure 27. MR swashplate equilibrium pitch in level flight – O50 calculation.

The same set of equilibrium data was provided respectively for steady autorotation conditions.

4.4.2. Near-ground maneuverers

Near-ground equilibrium was investigated in IGE hover with presence of wind acting from various azimuths. Figure 28 shows MR swashplate pitch for two skid heights over ground (3m – dashed line, 6m – solid line).

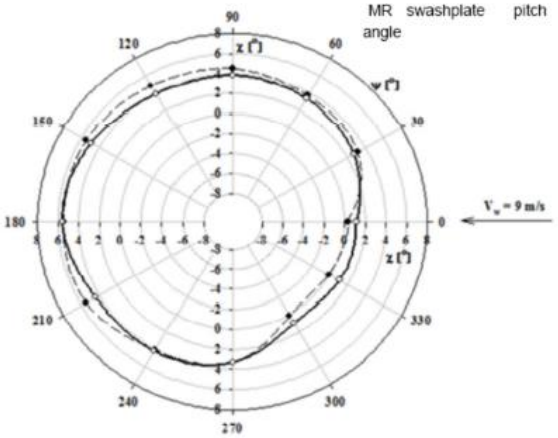

Figure 28. MR swashplate pitch in IGE hover.

Presented at 45th European Rotorcraft Forum, Warsaw, Poland, 17-20 September, 2019

4.4.3. Engine static performance

Engine sub-model validation was supported by static performance data. It was calculated with use of dedicated Rolls-Royce application. Ratings were evaluated for four cases: nominal and maximum continuous power turbine speed correlated with maximum continuous and take-off TOT limits. Additionally, performances corresponding with cold conditions flight tests were calculated.

4.5. Landings on a moving platform

WUT is to optimize h/c landing procedure on a vessel helideck. In order to provide a reasonable start point and reference, PZL provided flight tests data form trials of landing on a moving platform. It was performed by approaching to wheeled platform towed along airfield runway. Trials aimed in assess PZL SW-4 capabilities of performing automatic landing. Measurement data set is compliant with defined in 4.1.2.

Figure 29. Landing on a moving platform.

Measured signals were correlated with particular approaches to make them easier to interpret. Example of flight test data with distinguished approaches is shown on Figure 30. Following graphs represents signals 800.0, 801.0 911.3, 800.8, 811.8 (refer to Table 4). Additionally, video recording of each particular approach was provided.

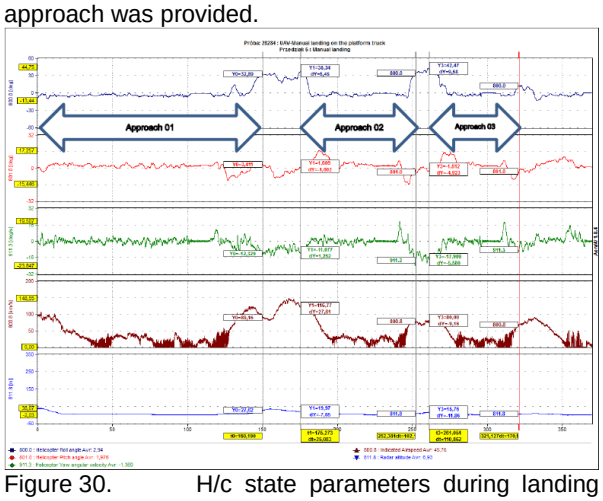

Figure 30. H/c state parameters during landing on a moving platform.

5. MODEL SIMILARITY CRITERIA

It is required to provide some objective criteria of dynamic model assessment. That would allow to verify if demanded similarity is achieved. PZL provided qualitative and quantitative criteria based on relative difference between model and h/c response and state at certain time. They were sorted in order of relevance:

a. Helicopter model response vector element signs should be the same as measured during flight tests at the beginning of free response phase.

b. Relative difference in dynamic response of the helicopter, defined as helicopter angular position (pitch, roll and yaw from Crossbow – measurement points 901.3, 900.3, 902.3), flight speed, altitude and angular speed at the time of 1s after beginning of free response phase should be not more than 10%.

c. Helicopter model response vector (position and time derivative) should follow the same time-dependence as measured in flight tests during free response phase.

6. AUTOPILOT SUB-MODEL

In scope of the HELIMARIS project, WUT would simulate autopilot system. That would allow to perform maritime missions autonomously, especially when it comes to more hazardous environmental conditions and flight states. This assumptions implies some specific autopilot requirements. Project would result in preliminary approach to system hardware design. General functional diagram is shown on Figure 31.

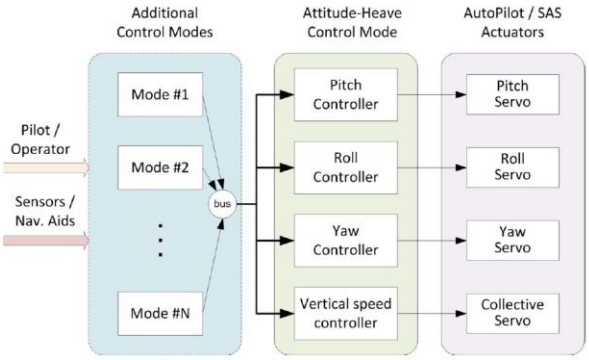

Figure 31. General autopilot functional diagram.

6.1. Functionality

System should demonstrate two main functionalities:

- stabilizing sub-system for ‘hands-on’ flying, which increase the short time attitude and attitude rate helicopter stability characteristics. It shall reduce short time responses of the helicopter on external disturbances in pitch, roll and yaw channels. Additionally, the system shall also reduce combination of roll and yaw motion to stabilize and improve turn coordination in automatic flight (development activity shall be focused on agreed flight conditions);
- 4-axis autopilot system providing automatic maneuvers realization by helicopter model; autopilot control algorithms shall allow to select requested flight task, to move helicopter controls to perform task and maintain flight path within established error

Presented at 45th European Rotorcraft Forum, Warsaw, Poland, 17-20 September, 2019

limitations (development activity shall be focused on automatic approaching and landing on ship deck).

6.2. Emergency scenarios

The system should allow to continue a mission in case of on-board sensors interruption (defined in Table 5) and unintentional floats inflation (symmetrical and unsymmetrical). PZL will provide floats aerodynamic characteristics. Additionally, influence of actuation tolerances, sensor data quality and autopilot authority would be investigated.

6.3. Requirements

The system should meet following requirements:

- automatic vertical take-off and landing on ship deck for sea state 5 with assistance of ship equipment and for sea state 4 without support from ship data;
- maintain the helicopter within the general limitations in approaching and landing on ship deck;
- manage the failures and emergency modes (unintended symmetrical and unsymmetrical floats opening resulting in instantaneous change of fuselage aerodynamic characteristics);
- shall be able to employ the following navigation parameters in case of support from ship sensors:
    - Wind Direction;
    - Wind Speed;
    - Magnetic Variation;
- shall implement the following general modes:
    - Dir-to (Fly-to);
    - Loiter - to be analyzed optionally;
    - Hover;
    - Land (waypoint associated to a Land procedure);
    - Take-off (waypoint associated to a Take-off procedure);
    - Follow ship/boat (maintain bearing and distance);
- shall be capable to manage an approach course to the waypoint expressed as angle between 0 and 359°;
- optionally, input data from optoelectronic head, SAR and/or LIDAR although ship position and helideck environmental parameters may be also included in mission control algorithm;
- the normal take-off and landing procedure profile shall be consistent with RFM sequence.

6.4. Limitations

The system should follow limitations refereeing to:

- transmission speed
- touch-down conditions;
- airspeed and groundspeed;
- speed of rotation in hover;
- torque safety margin;
- vortex ring protection;
- torque limits;
- H-V zone protection.

PZL provided estimated vortex ring envelope for PZL SW-4. It was based on general non-dimensional envelope[6], which was multiplied by average induced velocity in hover. Resulting graph is shown on Figure 32. Dashed line refers to small flight disturbances while solid line to heavy ones.
Vx – forward velocity;
Vy – descend velocity.

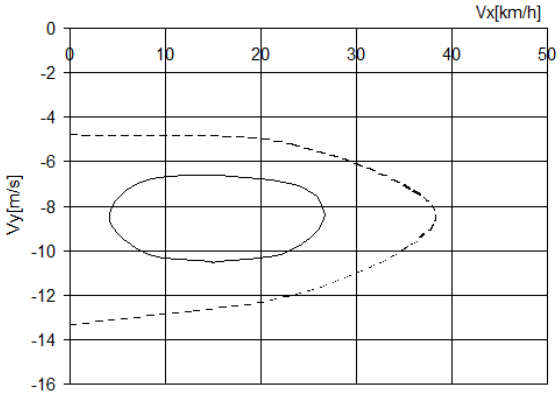

Figure 32. Estimated PZL SW-4 vortex ring envelope.

7. SUMMARY

The paper presents the entire set of data required to build h/c dynamic model in FLIGHTLAB environment. Input data was listed and necessary characteristics were presented. The most profound difficulties which occurred were highlighted. They originated mostly from significant modelling differences between currently used O50 code and FLIGHTLAB. Source of all data was provided as well as pre-processing methodology.
PZL prepared complete set of test results, necessary for validation of h/c model with all relevant sub-models. Definition of measured parameters was provided. Data is sufficient for dynamic identification in time domain in entire flight conditions envelope. Static equilibrium part declares final control elements position and performances, which model should comply with.
The paper contains also description of autopilot system, which is to be simulated after validation of basic h/c model is completed.
Finally, scope of further work required from PZL is stated, as far as proceeding with next steps of the project is considered. Papers referring to model development, validation, autopilot algorithms and objective assessment tool for simulator will be presented by WUT. Part of HELIMARIS project describing maritime environment modelling will be presented in separate papers.

Presented at 45th European Rotorcraft Forum, Warsaw, Poland, 17-20 September, 2019

8. ACKNOWLEDGEMENTS

Research conducted as part of the INNOLOT sector project (acronym HELIMARIS) entitled “Modification of an optionally piloted helicopter to maritime mission performance” coordinated by Wytwórnia Sprzętu Komunikacyjnego “PZL-Świdnik” Spółka Akcyjna, co-financed by the National Centre for Research and Development under the Smart Growth Operational Programme 2014-2020, 1. Priority Axis, Support for R&D activity of Enterprises; Action 1.2, Agreement No. POIR.01.02.00-00.0004/15.

Author would like to thank PZL colleagues involved in the project for their significant commitment in data preparation and advice. Especially, it is addressed to Ewa Janusz – Project Leader, Jacek Małecki – Head of Aero-mechanics Office and Radosław Raczyński – the other Work Package Leader. Furthermore, thanks are needed for WUT team lead by Ph. D. Przemysław Bibik, for their commitment in FLIGHTLAB input preparation and close cooperation in the project.

9. REFERENCES

[1]. Браверман А.С., Перлштейн Д.М., Лаписова С.В., *Балансировка одновинтового вертолета*, Машиностроение, Moscow 1975.

[2]. Bramwell A. R. S., Done G., Balmford D., *Bramwell’s Helicopter Dynamics*, Buttereworth-Heinemann, Oxford 2001.

[3]. Radosław Raczyński, *The use of CO-SIMULATION methodology in the project of PZL SW-4 helicopter adaptation to maritime version.*, 45th European Rotorcraft Forum 2019 (ERF), Warsaw, Poland.

[4]. Tischler M. B., Remple R. K, Schetz J. A., *Aircraft and Rotorcraft System Identification*, American Institute of Aeronautics and Astronautics, Reston 2012.

[5]. De Silva C. W., *Modeling of Dynamic Systems with Engineering Applications*, Taylor & Francis Group, Boca Raton 2018.

[6]. Szumański K., *Teoria i badania śmigłowców w ujęciu symulacyjnym*, Biblioteka Naukowa Instytutu Lotnictwa, Warszawa 1997.

APPENDIX
Appendix includes tables.

Presented at 45th European Rotorcraft Forum, Warsaw, Poland, 17-20 September, 2019

Table 1. Definition of the PZL SW-4 helicopter mass properties

Parameter definition	symbol	Unit	**CONF0**	**CONF1**	**CONF2**
Total helicopter weight	*G* / **vweight**	[kg]	Minimum	Medium	MTOW
OX CoG coordinate	x_T / **fscg**	[m]	Aft	Medium	Forward
OY CoG coordinate	y_T / **wlcg**	[m]	Top	Bottom	Bottom
OZ CoG coordinate	z_T / **blcg**	[m]	Neutral		
Total moment of inertia about OX	**ixx**	[kgm^2]	Resultant from h/c configuration.		
Total moment of inertia about OY	**iyy**	[kgm^2]			
Total moment of inertia about OZ	**izz**	[kgm^2]			
Total cross product OXY	**ixy**	[kgm^2]			
Total cross product OXZ	**ixz**	[kgm^2]			
Total cross product OYZ	**iyz**	[kgm^2]			

Table 2. Collective vs. Power lever kinematics [%].

Position of collective lever	Position of MR speed trimming stick	Collective lever travel from neutral	Collective angle at radius 0.7*Rw*	Power turbine lever angle
nominal	neutral	50	50	57
bottom	neutral	0	0	46
top	neutral	100	100	68
bottom	bottom	0	0	40
top	top	100	100	75

Table 3. Stabilizing surfaces input parameters.

	Horizontal stabilizer	Vertical stabilizer	End-plates
Reference area	*SSP*	*SKIL*	-
Chord	**hchord**	*BK* / **vchord**	**chord**
Span	**hlen**	**vlen**	**span**
Position	*OSPWN1, OSPWN, OLKIL* / **fsht, blht, wlht**	*ZSO, YKIL* / **fsvt, blvt, wlvt**	**fssurf, blsurf, wlsurf**
Orientation	**psithephisurf**	*EPSKIL* / **psithephisurf**	**psithephisurf**

Presented at 45th European Rotorcraft Forum, Warsaw, Poland, 17-20 September, 2019

Table 4. Listing of measured signals.

Meas. Point No.	Parameter Description	Abbreviation	Sampling Frequency/ Cut-off Filter Frequency
1	**2**	**3**	**7**
988.0	Main Rotor speed	N_r	0.04fs/-
988.1	Main Rotor speed (fast sampling)	N_{rfast}	fs/0.25fs
852.8	Engine output torque	M_o	fs/0.25fs
987.0	Engine gas generator speed	N_{ts}	fs/0.25fs
983.6	Engine turbine speed	N_{tn}	fs/0.25fs
602.6	Engine turbine outlet temperature	TOT	fs/0.25fs
800.8	Indicated airspeed	V_{IAS}	fs/0.25fs
801.8	Pressure altitude	H_b	fs/0.25fs
811.8	Radar altitude	H_g	fs/0.25fs
600.0	Ambient temperature	OAT	fs/0.25fs
501.3	MR swashplate pitch	χ	fs/0.25fs
500.3	MR swashplate roll	η	fs/0.25fs
502.3	MR collective (on r=0.7R)	φ_{07WN}	fs/0.25fs
503.3	TR collective (on r=0.7R)	φ_{07SO}	fs/0.25fs
505.0	1st blade MR blade lead – lag angle	ξ/I	4fs/0.25fs
504.0	1st blade MR blade flap angle	β/I	4fs/0.25fs
801.0	Helicopter fuselage pitch	υ	fs/0.25fs
800.0	Helicopter fuselage roll	γ	fs/0.25fs
920.1	Forward acceleration X -BK 4573	n_{x1}	fs/0.25fs
921.1	Vertical acceleration Y -BK 4573	n_{y1}	fs/0.25fs
922.1	Side acceleration Z -BK 4573	n_{z1}	fs/0.25fs
910.2	Helicopter roll speed X FED	ω_{x2}	fs/0.25fs
911.2	Helicopter yaw speed Y FED	ω_{y2}	fs/0.25fs
912.2	Helicopter pitch speed Z FED	ω_{z2}	fs/0.25fs
910.3	Helicopter roll speed X Crossbow	ω_{x3}	fs/0.25fs
911.3	Helicopter yaw speed Y Crossbow	ω_{y3}	fs/0.25fs
912.3	Helicopter pitch speed Z Crossbow	ω_{z3}	fs/0.25fs
900.3	Helicopter roll angle Crossbow	γ_3	fs/0.25fs
901.3	Helicopter pitch Crossbow	υ_3	fs/0.25fs
902.3	Helicopter yaw Crossbow	ψ_3	fs/0.25fs
920.3	Forward acceleration X Crossbow	n_{x3}	fs/0.25fs
921.3	Vertical acceleration Y Crossbow	n_{y3}	fs/0.25fs
922.3	Side acceleration Z Crossbow	n_{z3}	fs/0.25fs
802.0	Sideslip angle	β	fs/0.25fs
803.8	GPS N-S Latitude	x_{GPS}	Maximum accessible frequency of GPS messages
804.8	GPS W-E Longitude	z_{GPS}	
821.8	GPS Height	h_{GPS}	
818.8	GPS Speed	V_{GPS}	

Presented at 45th European Rotorcraft Forum, Warsaw, Poland, 17-20 September, 2019

Table 5. Input data interruption definition.

Unavailable data	**Flight state**
Failure 1	
A/C Forward True Airspeed	Level flight
Failure 2	
A/C altitude (Barometric and MSL)	Hover
A/C Vertical Speed	
Failure 3	
A/C Attitudes (Pitch, Roll, Heading)	Take-off
Engine/Transmission Speed	
Torque	

Presented at 45th European Rotorcraft Forum, Warsaw, Poland, 17-20 September, 2019